

UC Irvine

UC Irvine Previously Published Works

Title

Enhanced El Niño Southern Oscillation Variability in Recent Decades

Permalink

<https://escholarship.org/uc/item/1c77n951>

Journal

Geophysical Research Letters, 47(7)

ISSN

0094-8276 1944-8007

Authors

Grothe, Pamela R

Cobb, Kim M

Liguori, Giovanni

et al.

Publication Date

2020-04-04

DOI

10.1029/2019GL083906

Peer reviewed

Geophysical Research Letters

RESEARCH LETTER

10.1029/2019GL083906

Key Points:

- Line Island corals provide 1,751 years of monthly resolved ENSO variability from the mid-Holocene to present
- ENSO strength is significantly weaker between 3,000 and 5,000 years ago compared to the 2,000-year periods both before and after
- ENSO extremes of the last 50 years are significantly stronger than those of the preindustrial era in the central tropical Pacific

Supporting Information:

- Supporting Information S1

Correspondence to:

P. R. Grothe,
pgrothe@umw.edu

Citation:

Grothe, P. R., Cobb, K. M., Liguori, G., Di Lorenzo, E., Capotondi, A., Lu, Y., et al. (2019). Enhanced El Niño–Southern oscillation variability in recent decades. *Geophysical Research Letters*, 46, e2019GL083906. <https://doi.org/10.1029/2019GL083906>

Received 28 MAY 2019

Accepted 3 OCT 2019

Accepted article online 25 OCT 2019

Enhanced El Niño–Southern Oscillation Variability in Recent Decades

Pamela R. Grothe^{1,2} , Kim M. Cobb¹, Giovanni Liguori³, Emanuele Di Lorenzo¹ , Antonietta Capotondi⁴, Yanbin Lu⁵, Hai Cheng^{6,7}, R. Lawrence Edwards⁶, John R. Suthon⁸ , Guaciara M. Santos⁸ , Daniel M. Deocampo⁹ , Jean Lynch-Stieglitz¹ , Tianran Chen¹⁰ , Hussein R. Sayani¹, Diane M. Thompson¹¹ , Jessica L. Conroy¹² , Andrea L. Moore¹³, Kayla Townsend¹, Melat Hagos¹, Gemma O'Connor¹⁴, and Lauren T. Toth¹⁵ 

¹School of Earth and Atmospheric Sciences, Georgia Institute of Technology, Atlanta, GA, USA, ²Now at the Department of Earth and Environmental Sciences, University of Mary Washington, Fredericksburg, VA, USA, ³ARC Centre of Excellence for Climate Extremes, and School of Earth, Atmosphere and Environment Monash University, Melbourne, Victoria, Australia, ⁴NOAA, Earth System Research Laboratory, Physical Sciences Division, Boulder, CO, USA, ⁵Institute of Earth Environment Chinese Academy of Sciences, Xi'an, USA, ⁶Department of Earth Sciences, University of Minnesota, Minneapolis, MN, USA, ⁷Institute of Global Environmental Change, Xi'an Jiaotong University, Xi'an, China, ⁸Department of Earth System Science, University of California, Irvine, CA, USA, ⁹Department of Geosciences, Georgia State University, Atlanta, GA, USA, ¹⁰South China Sea Institute of Oceanology, Chinese Academy of Sciences, Guangzhou, China,

¹¹Department Geosciences, University of Arizona, Tucson, AZ, USA, ¹²Department of Geology and Department of Plant Biology, University of Illinois at Urbana-Champaign, Urbana, IL, USA, ¹³Department of Earth and Environmental Sciences, University of Mary Washington, Fredericksburg, VA, USA, ¹⁴Department of Earth and Space Sciences, University of Washington, Seattle, WA, USA, ¹⁵U.S. Geological Survey, St. Petersburg Coastal and Marine Science Center, St. Petersburg, FL, USA

Abstract The El Niño–Southern Oscillation (ENSO) represents the largest source of year-to-year global climate variability. While Earth system models suggest a range of possible shifts in ENSO properties under continued greenhouse gas forcing, many centuries of preindustrial climate data are required to detect a potential shift in the properties of recent ENSO extremes. Here we reconstruct the strength of ENSO variations over the last 7,000 years with a new ensemble of fossil coral oxygen isotope records from the Line Islands, located in the central equatorial Pacific. The corals document a significant decrease in ENSO variance of ~20% from 3,000 to 5,000 years ago, coinciding with changes in spring/fall precessional insolation. We find that ENSO variability over the last five decades is ~25% stronger than during the preindustrial. Our results provide empirical support for recent climate model projections showing an intensification of ENSO extremes under greenhouse forcing.

Plain Language Summary Recent modeling studies suggest that El Niño will intensify due to greenhouse warming. Here new coral reconstructions of the El Niño–Southern Oscillation (ENSO) record sustained, significant changes in ENSO variability over the last 7,000 years and imply that ENSO extremes of the last 50 years are significantly stronger than those of the preindustrial era in the central tropical Pacific. These records suggest that El Niño events already may be intensifying due to anthropogenic climate change.

1. Introduction

El Niño–Southern Oscillation (ENSO) extremes have a profound impact on global temperature and rainfall patterns, driving costly floods and droughts in many regions of the world. Warm ocean temperatures during strong El Niño events during 1997/1998 and 2015/2016 (Figure 1) caused widespread coral bleaching and mortality across the tropical oceans (Wake, 2016; Wilkinson, 2004). Climate models project a variety of changes in ENSO properties that, taken together, would increase the impact of ENSO extremes on communities and ecosystems around the world under continued greenhouse forcing (Cai et al., 2014; Cai et al., 2015; Cai et al., 2018; Collins et al., 2010). The recent spate of large El Niño events (1982/1983, 1997/1998, and 2015/2016) raises the prospect that climate change may already be contributing to an intensification of ENSO extremes. However, the small number of ENSO extremes captured in the decades-long instrumental climate record precludes the detection of robust trends in ENSO properties. Reconstructions of past ENSO

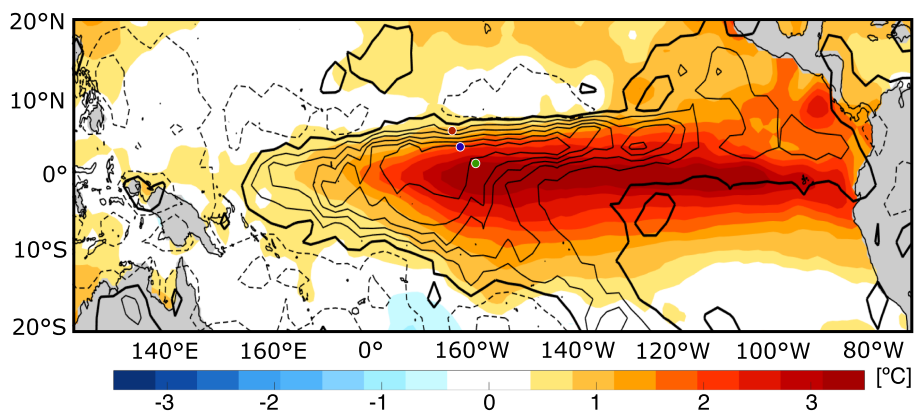


Figure 1. Map of tropical Pacific temperature and precipitation anomalies at the peak of the 2015/2016 El Niño event. Sea surface temperature (color shading; Reynolds et al., 2002) and precipitation (contours; Xie & Arkin, 1997) anomalies during the November–December–January average. Contour spacing is 2 mm/day, and the thick solid line represents the 0 anomaly, which separates positive (solid lines) and negative (dashed lines) anomalies. Green dot denotes the location of Kiritimati (Christmas) Island (2°N , 157°W); blue dot denotes the location of Fanning Island (4°N , 160°W); and red dot denotes the location of Palmyra Island (6°N , 162°W).

variability based on paleoclimate archives provide quantitative estimates of ENSO properties in the preindustrial era, resolving ENSO properties under a variety of natural climate forcing scenarios (Carré et al., 2014; Cobb et al., 2013; Conroy et al., 2008; Koutavas & Joanides, 2012; Moy et al., 2002; Rodbell et al., 1999; White et al., 2018). As such, they serve as much-needed baselines for natural ENSO variability, as well as out-of-sample tests for climate model simulations of ENSO's response to past external climate forcing.

One of the most relevant tests of ENSO's sensitivity to external forcing comes from the Holocene (the last 10,000 years), when a suite of modeling studies (Clement et al., 2000; Liu et al., 2000, 2014; Otto-Bliesner et al., 2003; Timmermann et al., 2007; Zheng et al., 2008) suggest that a decrease in the amplitude of the seasonal insolation cycle from the early to late Holocene led to a progressive intensification of ENSO variability. However, while some reconstructions of Holocene ENSO supported this framework (Conroy et al., 2008; Moy et al., 2002; Rodbell et al., 1999; White et al., 2018), several recent studies do not show any significant reduction in ENSO variance during the early Holocene (Carré et al., 2014; Cobb et al., 2013; Koutavas & Joanides, 2012). A review of available Holocene paleo-ENSO reconstructions from across the tropical Pacific suggests that ENSO may have been somewhat reduced 3,000–5,000 years before present (kyr BP; Emile-Geay et al., 2016), although the limited nature of the paleo-ENSO datasets available at the time precluded any robust statistical analyses. Indeed, both models and data underscore the high level of intrinsic ENSO variability, raising the bar for the detection of forced changes in ENSO, whether natural or anthropogenic.

Fossil coral records from the central tropical Pacific provide high-fidelity paleo-ENSO reconstructions owing to their location in the heart of the ENSO region, their monthly resolution, and their demonstrated sensitivity to ENSO-related changes in sea surface temperature (SST; Cobb et al., 2003; McGregor, Fischer, et al., 2013). Indeed, coral oxygen isotopic ($\delta^{18}\text{O}$) records from Palmyra (6°N , 162°W), Fanning (4°N , 160°W), and Kiritimati (Christmas) Island (2°N , 157°W) closely track variations in the NIÑO3.4 SST index (see Figure S9), a key ENSO metric, as warm, rainy conditions during El Niño events drive coral $\delta^{18}\text{O}$ lower and vice versa during cool, dry La Niña conditions (Cobb et al., 2013). In this study, we present 16 new monthly resolved fossil coral $\delta^{18}\text{O}$ sequences from Kiritimati Island whose U/Th dates span from 2.5 to 5.2 kyr BP, as well as an updated modern coral spliced record from both Kiritimati and Palmyra Islands, now spanning from 1938–2016 CE and 1886–2007 CE, respectively. The modern spliced records, which are the basis for subsequent analyses of ENSO variance changes, are created from overlapping oxygen isotopic records from living corals drilled on the reef (see supporting information S1), which at Kiritimati Island show good reproducibility across multiple cores and demonstrate that local changes in SST are the primary driver of coral $\delta^{18}\text{O}$ departures (Figure 2). The new fossil sequences range from 7 to 26 years in length, for a

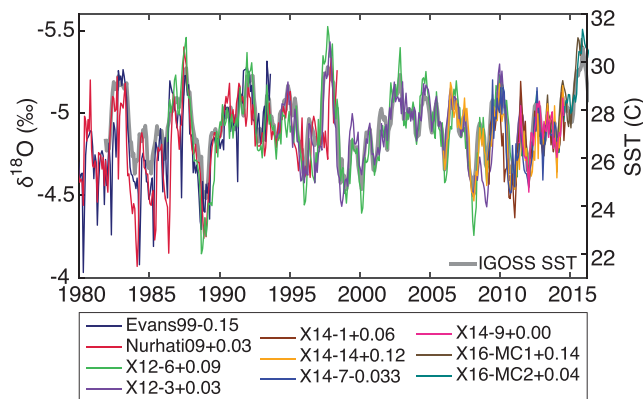


Figure 2. Ten monthly resolved coral $\delta^{18}\text{O}$ records from living corals drilled from Kiritimati Island plotted with Integrated Global Ocean Services System (IGOSS) sea surface temperature (SST; Reynolds et al., 2002) from the gridbox containing Kiritimati Island (gray). Each coral record has been shifted by up to 0.15‰ to match the mean $\delta^{18}\text{O}$ values in overlapping intervals of the records to create a stack of all overlapping records, with offsets in per mil reported in legend (see Figure S2). Corals from left to right include Evans et al. (1999; navy); Nurhati et al. (2009; crimson); this study, X12-6 (emerald) and X12-3 (purple); X14-1 (sienna), X14-14 (orange), X14-7 (blue) and X14-9 (hotpink; T. Chen, pers. comm.); and X16-MC1 (brown) and X16-MC2 (teal; G. O'Connor, pers. comm.). For the purposes of statistical analyses presented in this study, a composite coral $\delta^{18}\text{O}$ record was created by splicing individual coral sequences together.

not included in the final coral $\delta^{18}\text{O}$ time series. The coral $\delta^{18}\text{O}$ analyses were conducted on powders drilled at 1 mm increments, following standard procedures for coral core slabbing and cleaning. Long-term reproducibility for the Thermo-Finnigan Delta V-Kiel at Georgia Tech is better than ± 0.07 per mil ($1\sigma, N > 1,000$).

2. ENSO Variability During Middle to Late Holocene

To assess relative changes in ENSO variance across the Line Islands coral reconstructions, fossil coral interannual variability changes are benchmarked against recent coral interannual variability estimates, quantified from the modern spliced records from the corresponding site to account for differing ENSO amplitudes across the islands. We note that the structure of ENSO across these sites has not changed during the instrumental era. To account for many of the samples short segment length, we quantify interannual variability as the standard deviation of 10-year high-passed, 13-month running mean versions of the time series, reported as the average standard deviation in sliding 20-year windows back through time, relative to a 1987–2007 reference period. The 20-year window length employed in our analyses is designed to match the length of most fossil coral sequences, though we also repeat our analyses using a range of window lengths (see Figure S18). The 1987–2007 reference period was selected as it represents the most recent period for which coral $\delta^{18}\text{O}$ data exist from Kiritimati, Palmyra, and Fanning Islands. While our analyses and associated results are broadly comparable to those presented in Cobb et al. (2013), the addition of 233 years of data, combined with the use of an improved set of ENSO time series chosen as null hypotheses, leads to a more robust detection of changes in ENSO variance that represent departures from our best estimates of stationary ENSO variability.

The new coral archive reveals a large range of interannual variance, from -77% roughly 4,200 years ago to $+18\%$ roughly 260 years ago, relative to the 1987–2007 reference period, well within the range of previously published data from the Line Islands (Figure 3; Cobb et al., 2013). In any given millennium, interannual variance is highly variable. Although segment length contributes some uncertainty to these variance estimates, these results provide support for a high degree of intrinsic variability as a perennial feature of late Holocene ENSO and provide a quantitative benchmark for data-model comparisons. By comparison, changes in ENSO variance over the last 120 years are relatively muted, ranging from a low of -45% in 1944–1964 to $+8\%$ in 1980–2000, relative to the 1987–2007 reference period (see Figure S9). It is worth noting that the vast

total of 233 years of new monthly resolved paleo-ENSO data (see Figure S2 and Table S2). These new sequences, in combination with previously published coral sequences from Christmas, Fanning, and Palmyra Islands (Cobb et al., 2013; McGregor, Fischer, et al., 2013), now total 1,751 years from 38 fossil coral sequences from $\sim 7,000$ years ago through to the record-breaking 2016 El Niño event. The longest fossil sequence is 318 years long (1147 to 1465 CE) and represents a combination of previously published data from Cobb et al. (2003) and new data presented in Dee et al. (n.d.). This new dataset from the Line Islands allows us to identify more subtle changes in ENSO variance over the middle to late Holocene that can be tested against estimates of internal ENSO variability as represented in long model-derived time series of ENSO variability.

We carefully screen each new coral sequence for alteration using scanning electron microscopy, X-ray diffraction, and by testing for concordance between rapid-screen radiocarbon (^{14}C) and Uranium-thorium (U/Th) dates (Grothe et al., 2016). X-ray diffraction analyses revealed no detectable calcite ($<0.5\%$), while scanning electron microscopy images revealed evidence of trace to minor alteration characterized by small discontinuous patches of secondary aragonite crystals ($<10 \mu\text{m}$) and/or minor dissolution (see Figure S6; Cobb et al., 2013; Sayani et al., 2011). Sections of the corals that contained diagenetic alteration, which were typical of the core tops and bottom, were

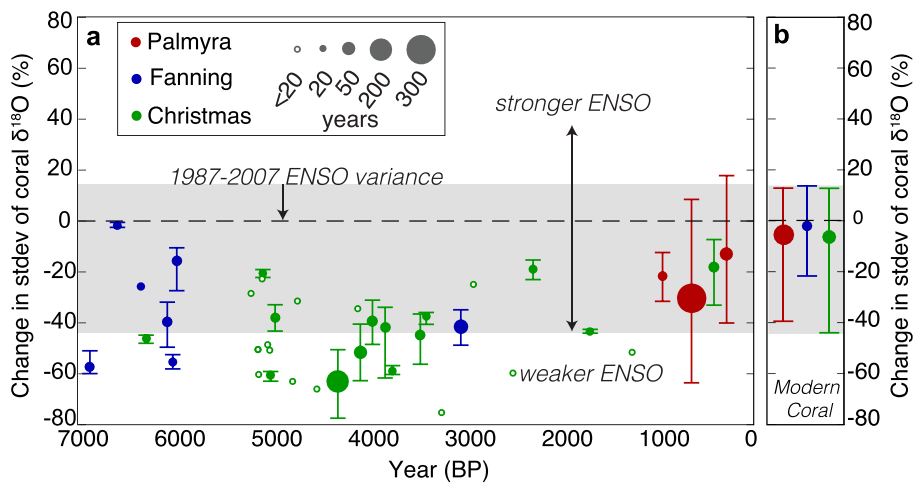


Figure 3. Estimates of interannual variability from new and published coral $\delta^{18}\text{O}$ records from the northern Line Islands. (a) Relative El Niño–Southern Oscillation (ENSO) variance changes in fossil coral $\delta^{18}\text{O}$ calculated from the standard deviation of sliding 20-year windows of monthly coral $\delta^{18}\text{O}$ data that was first 10-year high passed, then 13-month running averaged, plotted as the average standard deviation of each coral time series relative to the 1987–2007 CE intervals of corresponding modern spliced coral $\delta^{18}\text{O}$ time series from each site (the dashed “zero” line). Coral data originate from Palmyra (red; Cobb et al., 2003), Fanning (blue; Cobb et al., 2013), and Kiritimati (green; Cobb et al., 2013; McGregor, Fischer, et al., 2013; and this study). The bars represent the full range of interannual variability in 20-year windows of each coral sequence. Coral time series of <20 years are plotted with open circles. Coral time series from 20 years < length < 320 years are plotted linearly with size where smaller dots are shorter sequences. The gray box denotes the full range of ENSO variability from the modern spliced coral records in 20-year windows, as reflected in panel (b). (b) Same as in (a) but for the modern spliced coral $\delta^{18}\text{O}$ time series for each island (Palmyra: 1886–2007 CE; Fanning 1949–2005 CE; Kiritimati Island: 1939–2016 CE). Colors as in (a).

majority of the fossil coral-based estimates of interannual variability (70 of 72 nonoverlapping 20-year-long segments) falls below that of the 1987–2007 reference period. In particular, a multmillennium period centered at 4,000 years ago stands out as an episode marked by dramatically reduced interannual variability, an observation made possible by doubling the data coverage in this time interval, relative to data presented in Cobb et al. (2013; Figure 3). Indeed, estimates of interannual variance from 3- to 5-kyr BP averages -49% relative to the 1987–2007 benchmark, as compared to -37% in the 5- to 7-kyr BP and -30% in the 0- to 2-kyr BP intervals.

Given the sparse temporal coverage of the coral reconstruction, it is important to understand whether the observed changes in interannual variance reflect real changes in the expression of ENSO or simply result from undersampling a highly variable system. To that end, we test the null hypothesis that the changes in variance observed across the coral archive fall within the range of intrinsic ENSO variability estimated from two simulations of long-term ENSO variability. The first null hypothesis for long-term ENSO variability comes from a statistical linear inverse model (LIM) trained on instrumental data from the 1958–2007 period and run for 20,000 years with stochastic noise (Capotondi & Sardeshmukh, 2017). The second null hypothesis utilizes output from the National Center for Atmospheric Research–Community Earth System Model—a fully coupled climate model—consisting of ten 1,000-year long simulations forced with solar and volcanic radiative perturbations (the Last Millennium Ensemble [LME]; Otto-Bliesner et al., 2015). In both cases, we use the respective NIÑO3.4 SST time series as indices of ENSO variability. These choices of null hypotheses are well suited to the statistical analyses presented herein and represent a significant improvement over those employed in Cobb et al. (2013), which were only 1,000–2,000 years in duration. A bootstrap approach is then used to randomly extract 10,000 pseudo-coral reconstructions from the long LIM and LME NIÑO3.4 time series, preserving the number and length of the real coral time series for each pseudo-coral dataset. While it is impossible to know if the LIM and LME accurately represent the range of ENSO variance over many millennia, their ENSO variance distributions are consistent with preindustrial coral data, given the uncertainties associated with such a comparison (see Figure S11). We infer that, by choosing two very

different types of data sets for our null hypothesis testing, we have applied the most stringent test available for identifying potentially forced changes in ENSO variability observed in the new coral archive.

To compute the significance testing, we randomly drew 10,000 different pseudo-coral datasets that are equivalent in number and length to the real coral dataset between 3 and 5 kyr BP and computed the relative change in standard deviation to another randomly drawn dataset of pseudo-corals that represents the number and length to the real coral datasets between both 5–7 and 0–2 kyr BP. We plot the distribution of these pseudo-coral-derived differences in variance between these epochs and denote the 95% and 99% confidence thresholds. In this way, if the observed difference in ENSO variance between the two epochs falls outside the 95% or 99% distribution limits derived from the bootstrap analyses, we describe that observed change in ENSO variance as not statistically consistent with our null hypotheses. The significance testing shows that the 3- to 5-kyr BP reduction in interannual variance is statistically significant (>99% confidence) for both choices of null hypotheses (Figures 4a–4d), a result that was not detectable in previous Line Islands datasets (Cobb et al., 2013). These results add to the growing body of paleo-ENSO records that show the strongest ENSO reduction around 4 kyr BP with higher variance in amplitude both before and after the long quiescent period (Emile-Geay et al., 2015). These archives include both $\delta^{18}\text{O}$ records from mollusk shells (Carré et al., 2014) and foraminifera (Koutavas & Joanides, 2012) and geochemical records from lake sediments (Thompson et al., 2017) from the eastern tropical Pacific as well as a stalagmite $\delta^{18}\text{O}$ record from Borneo (Chen et al., 2016). These independent lines of evidence support a basin-wide reduction in ENSO variance from ~4 kyr BP, possibly through a decrease in the underlying SST variance and/or a reduction of ENSO-related hydrological variability rather than a shift in the spatial footprint of ENSO (Karamperidou et al., 2015). However, recent work using central tropical Pacific SST reconstructions from foraminifera find evidence for reduced ENSO variability in the 5- to 7-kyr BP interval, (White et al., 2018), in apparent conflict with the findings from this study. The records' discrepancies may be reconciled by recognizing the potential role for decadal- to centennial-scale temperature variability in contributing to the changes in the absolute paleo-temperature distributions presented in White et al. (2018). Of course, the 5–7 kyr BP is the most data-sparse period of our reconstruction, so additional coral samples may reveal a more significant reduction in ENSO variance during this period. Indeed, the weighted mean for ENSO variance during the 5–7 kyr BP section is $-36\% \pm 4\%$, relative to the 1987–2007 CE benchmark, as compared to 3–5 kyr BP section at $-52\% \pm 4\%$. More so, these record-to-record differences illustrate that more basin-wide reconstructions are needed to reconcile the discrepancies among datasets.

A prolonged reduction in ENSO variance at 3–5 kyr BP may reflect a dynamical response to precessional forcing in boreal fall and spring, which coincide with ENSO's strongest growth and decay phases, respectively. However, climate models exhibit a significant sensitivity to summer/winter insolation, whereby an increase in the amplitude of the annual cycle across the equatorial Pacific (Braconnot et al., 2012; Clement et al., 2000; Liu et al., 2000; Zheng et al., 2008) and/or a reduction in subsurface temperature (Liu et al., 2014) drives a marked reduction in ENSO variance (Braconnot et al., 2012; Clement et al., 2000; Liu et al., 2000; Zheng et al., 2008). As such, the prolonged change in ENSO variance from 3–5 kyr BP—implying spring/fall sensitivity—represents a compelling target for coupled model simulations, with important implications for long-term ENSO predictability. Of course, the observed reduction in ENSO variance from 3–5 kyr BP may just as well reflect unforced variability in the coupled system, whose long-term variability, including potential cross-basin interactions, remain poorly constrained.

3. ENSO Variability in Recent Decades

One striking feature of the new reconstruction is that almost all of the preindustrial coral sequences reflect interannual variability, that is, on average, roughly 39% lower than the 1987–2007 reference period. When subject to the significance testing previously outlined, interannual variance over the last 50 years (1966–2016; quantified using data from each of the islands spliced modern coral record) is significantly (>95% confidence) higher than the preindustrial era (quantified using all of the fossil coral data that predate 1850), for both choices of null hypotheses (Figures 4e and 4f). In fact, our analyses reveal a statistically significant increase in interannual variability from the preindustrial to recent, whether the latter is defined by the previous 30, 50, 75, or 100 years before 2016 (see Figure S13). Interannual variability is relatively high in the early 1900's (see Figure S9), but it is not significantly higher than preindustrial levels (see Figure S15).

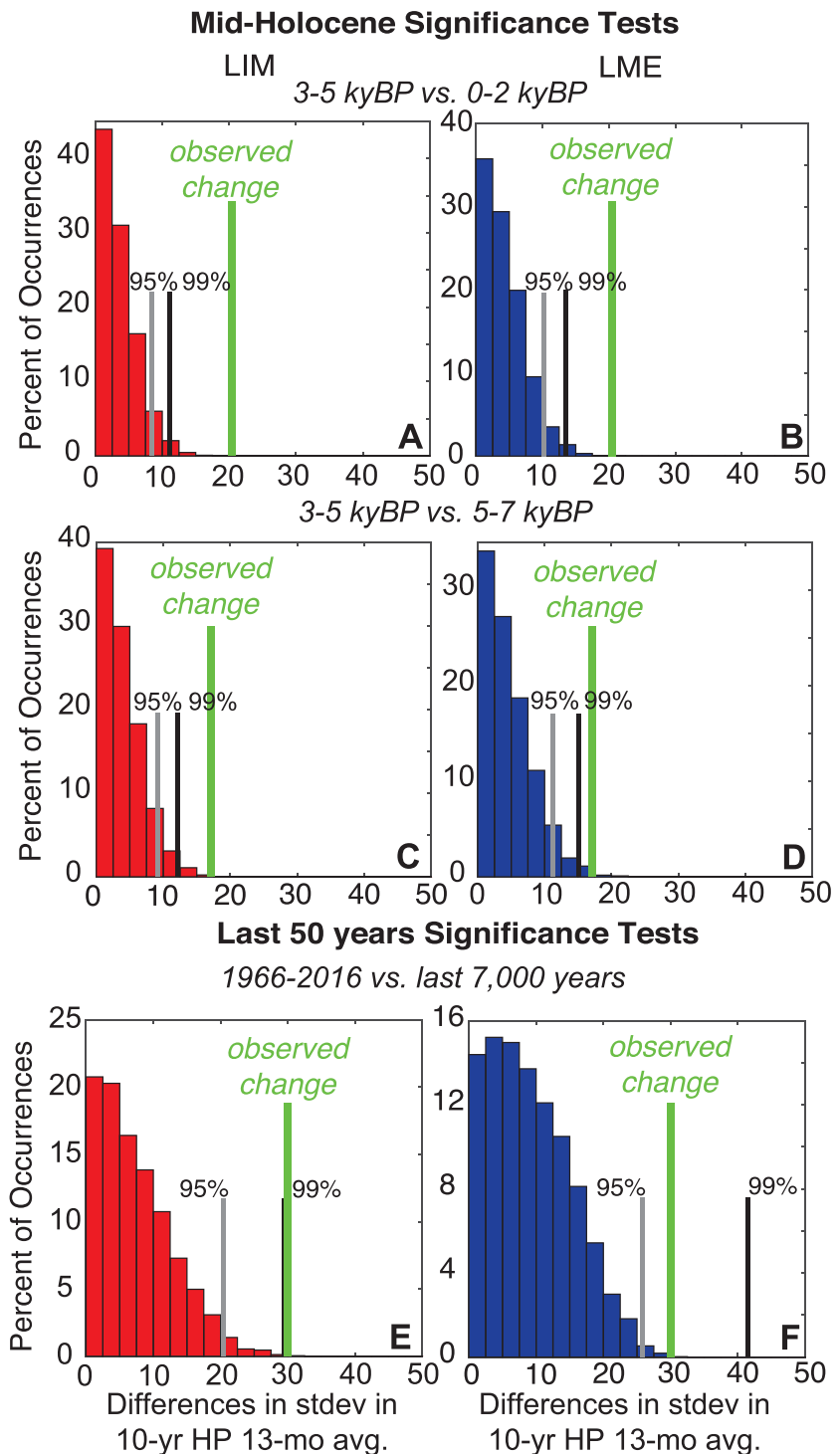


Figure 4. Results of significance testing for the observed differences in interannual variability of coral $\delta^{18}\text{O}$ over last 7,000 years. (a) Probability density function and significance levels (95% and 99%; gray and black lines, respectively) of differences between interannual variance in 10,000 pseudo-coral datasets designed to replicate the segment lengths of the 3- to 5-kyr BP Line Islands fossil coral data and the 0- to 2-kyr BP fossil coral data, generated from NI $\tilde{\text{N}}$ O3.4 time series from a linear inverse model (LIM) of ENSO (Capotondi & Sardeshmukh, 2017). The observed difference in interannual variance between the 3- to 5-kyr BP and 0- to 2-kyr BP fossil coral data is denoted by the green line. (b) Same as in (a) but pseudo-coral data are generated from NI $\tilde{\text{N}}$ O3.4 time series from the Last Millennium Ensemble (LME; Otto-Bliesner et al., 2016). (c) Same as in (a) but targeted at the 3–5 kyr BP versus 5–7 kyr BP fossil coral data. (d) Same as in (c) but pseudo-coral data are generated from the LME. (e) Same as in (a) but targeted at the difference between the last 50 years of coral data (1966–2016 CE) versus the entire Line Islands fossil coral dataset, with pseudo-coral data generated from the LIM. (f) Same as (e) but pseudo-coral data generated from the LME.

The recent intensification of interannual variability remains significant even if all 3- to 5-kyr BP data are removed from the preindustrial dataset—assuming they may reflect a forced decrease in ENSO variance (see Figure S14). Using the most recent millennium of data only, we find that the last 50-year ENSO variance is 25% stronger (>95% confidence) than the last millennium (see Figure S16). However, with the removal of the record-breaking 1997/1998 El Niño event from the modern spliced coral dataset, we find no significant increase in recent interannual activity (see Figure S17). While there is no a priori reason to exclude this event from our analysis, this finding does illustrate that we may have only recently exceeded the detection limit for observing enhanced variability in ENSO properties, as measured against long-term ENSO variability.

This study bolsters results from other long, multicentury reconstructions of ENSO that detect enhanced ENSO variability in the late twentieth century relative to the preindustrial period (Li et al., 2013; Liu et al., 2017; McGregor, Timmermann, et al., 2013). Models project an increased frequency of extreme El Niño events under continued greenhouse forcing linked to a slowdown in the Walker Circulation, weaker Pacific equatorial currents, and an associated strengthening of eastward-propagating warm SST anomalies (Cai et al., 2015). Indeed, a recent study uncovers a significant increase in ENSO-related SST variability in climate models under greenhouse forcing (Cai et al., 2018). Models also provide robust evidence for an enhanced hydrological response to El Niño events under anthropogenic forcing scenarios (Cai et al., 2014, 2015; Power et al., 2013), which may contribute to the increased ENSO variability observed in paleo-ENSO reconstructions, most of which reflect a contribution from hydrological variability. However, our results imply that interannual coral $\delta^{18}\text{O}$ variability at Kiritimati Island is almost entirely driven by interannual SST variability (Figure 2), such that the ~25% increase in interannual coral $\delta^{18}\text{O}$ variability very likely reflects an increase in ENSO-related SST variability. That said, our results may indicate a recent intensification of central tropical Pacific ENSO SST extremes, consistent with results from a recent analysis of multicentury coral records spanning the Indo-Pacific basin (Freund et al., 2019).

4. Implications for Future ENSO Variability

The new coral data document sustained, significant changes in ENSO properties: a weakening from 3–5 kyr BP potentially linked to spring/fall insolation and an intensification in recent decades possibly related to anthropogenic climate change. These observations are enabled by the addition of new coral $\delta^{18}\text{O}$ records to the Line Islands coral archive and by the availability of multimillennium representations of ENSO's internal variability to form robust null hypotheses. Both findings are supported by a number of recent paleo-ENSO reconstructions and as such represent high-priority targets for future investigations with numerical climate models. While the chain of dynamical feedbacks responsible for the observed changes in ENSO, past and present, remains unclear, the prospect for larger ENSO extremes under continued greenhouse forcing likely increases the societal and ecological vulnerabilities to climate change. As such, regional climate impact assessments of climate vulnerabilities that incorporate information from paleoclimate studies of climate extremes are needed in order to accurately assess the risks of continued anthropogenic-induced climate change.

References

- Braconnot, P., Luan, Y., Brewer, S., & Zheng, W. (2012). Impact of Earth's orbit and freshwater fluxes on Holocene climate mean seasonal cycle and ENSO characteristics. *Climate Dynamics*, 38(5–6), 1081–1092. <https://doi.org/10.1007/s00382-011-1029-x>
- Cai, W., Borlace, S., Lengaigne, M., van Rensh, P., Collins, M., Vecchi, G., et al. (2014). Increasing frequency of extreme El Niño events due to greenhouse warming. *Nature Climate Change*, 4(2), 111–116. <https://doi.org/10.1038/nclimate2100>
- Cai, W., Santoso, A., Wang, G., Yeh, S.-W., An, S.-I., Cobb, K. M., et al. (2015). ENSO and greenhouse warming. *Nature Climate Change*, 5(9), 849–859. <https://doi.org/10.1038/nclimate2743>
- Cai, W., Wang, G., Dewitte, B., Wu, L., Santoso, A., Takahashi, K., et al. (2018). Increased variability of eastern Pacific El Niño under greenhouse warming. *Nature*, 564(7735), 201–206. <https://doi.org/10.1038/s41586-018-0776-9>
- Capotondi, A., & Sardeshmukh, P. D. (2017). Is El Niño really changing? *Geophysical Research Letters*, 44, 8548–8556. <https://doi.org/10.1002/2017GL074515>
- Carré, M., Sachs, J. P., Purca, S., Schauer, A. J., Braconnot, P., Falcón, R. A., et al. (2014). Holocene history of ENSO variance and asymmetry in the eastern tropical Pacific. *Science*, 345(6200), 1045–1048. <https://doi.org/10.1126/science.1252220>
- Chen, S., Hoffmann, S. S., Lund, D. C., Cobb, K. M., Emile-Geay, J., & Adkins, J. F. (2016). A high-resolution speleothem record of western equatorial Pacific rainfall: Implications for Holocene ENSO evolution. *Earth and Planetary Science Letters*, 442, 61–71. <https://doi.org/10.1016/j.epsl.2016.02.050>
- Clement, A. C., Seager, R., & Cane, M. A. (2000). Suppression of El Niño during the Mid-Holocene by changes in the Earth's orbit. *Paleoceanography*, 15(6), 731–737. <https://doi.org/10.1029/1999PA000466>

Acknowledgments

The authors acknowledge the Republic of Kiribati for allowing research activities on Kiritimati Island through permits from 2012 and 2013 (number 005/13) provided by the Environment and Conservation Division. We thank Tiito Teabi for expert field support on numerous expeditions to Kiritimati from 2012 to 2016. This research was funded by National Science Foundation Awards 1502832 and 1446343 to K. M. C, National Science Foundation of China Award 41888101 to H. C., National Science Foundation Awards 1029020 and 1349599 to D. M. D., NOAA's Climate Program Office and DOE's Office of Science to A. C., National Science Foundation Award 1931242 to D. M. T., U.S. Geological Survey and National Science Foundation Award 1535007 to L. T. T., and Sigma Delta Epsilon-Graduate Women in Science fellowship to P. R. G. All data and metadata are archived at NCDC (<https://www.ncdc.noaa.gov/paleo/study/22415>). Any use of trade, firm, or product names is for descriptive purposes only and does not imply endorsement by the United States Government.

- Cobb, K. M., Charles, C. D., Cheng, H., & Edwards, R. L. (2003). El Niño/Southern Oscillation and tropical Pacific climate during the last millennium. *Nature*, 424(6946), 271–276. <https://doi.org/10.1038/nature01779>
- Cobb, K. M., Westphal, N., Sayani, H. R., Watson, J. T., Di Lorenzo, E., Cheng, H., et al. (2013). Highly variable El Niño–Southern Oscillation throughout the Holocene. *Science*, 339(6115), 67–70. <https://doi.org/10.1126/science.1228246>
- Collins, M., An, S.-I., Cai, W., Ganachaud, A., Guilyardi, E., Jin, F.-F., et al. (2010). The impact of global warming on the tropical Pacific Ocean and El Niño. *Nature Geoscience*, 3(6), 391–397. <https://doi.org/10.1038/geo868>
- Conroy, J. L., Overpeck, J. T., Cole, J. E., Shanahan, T. M., & Steinitz-Kannan, M. (2008). Holocene changes in eastern tropical Pacific climate inferred from a Galápagos lake sediment record. *Quaternary Science Reviews*, 27(11–12), 1166–1180. <https://doi.org/10.1016/j.quascirev.2008.02.015>
- Dee, S. G., Cobb, K. M., Emile-Geay, J., Ault, T. R., Edwards, R. L., & Cheng, H. (n.d.). Multi-century fossil corals reveal large thresholds for aerosol forcing impacts on the tropical Pacific. Submitted to *Science* on 03/05/2019.
- Emile-Geay, J., Cobb, K. M., Carré, M., Braconnot, P., Leloup, J., Zhou, Y., et al. (2015). Links between tropical Pacific seasonal, interannual and orbital variability during the Holocene. *Nature Geoscience*, 9(2), 168–173. <https://doi.org/10.1038/geo2608>
- Evans, M. N., Fairbanks, R. G., & Rubenstone, J. L. (1999). The thermal oceanographic signal of El Niño reconstructed from a Kiritimati Island coral. *Journal of Geophysical Research*, 104(C6), 13,409–13,421. <https://doi.org/10.1029/1999JC900001>
- Freund, M. B., Henley, B. J., Karoly, D. J., McGregor, H. V., Abram, N. J., & Dommgenet, D. (2019). Higher frequency of Central Pacific El Niño events in recent decades relative to past centuries. *Nature Geoscience*, 12(6), 450–455. <https://doi.org/10.1038/s41561-019-0353-3>
- Grothe, P. R., Cobb, K. M., Bush, S. L., Cheng, H., Santos, G. M., Southon, J. R., et al. (2016). A comparison of U/Th and rapid-screen 14C dates from Line Island fossil corals. *Geochemistry, Geophysics, Geosystems*, 17, 833–845. <https://doi.org/10.1002/2015GC005893>
- Karamperidou, C., Di Nezio, P. N., Timmermann, A., Jin, F.-F., & Cobb, K. M. (2015). The response of ENSO flavors to mid-Holocene climate: Implications for proxy interpretation. *Paleoceanography*, 30, 527–547. <https://doi.org/10.1002/2014PA002742>
- Koutavas, A., & Joanides, S. (2012). El Niño–Southern Oscillation extrema in the Holocene and Last Glacial Maximum. *Paleoceanography*, 27, PA4208. <https://doi.org/10.1029/2012PA002378>
- Li, J., Xie, S.-P., Cook, E. R., Morales, M. S., Christie, D. A., Johnson, N. C., et al. (2013). El Niño modulations over the past seven centuries. *Nature Climate Change*, 3(9), 822–826. <https://doi.org/10.1038/nclimate1936>
- Liu, Y., Cobb, K. M., Song, H., Li, Q., Li, C.-Y., Nakatsuka, T., et al. (2017). Recent enhancement of central Pacific El Niño variability relative to last eight centuries. *Nature Communications*, 8, 15386. <https://doi.org/10.1038/ncomms15386>
- Liu, Z., Kutzbach, J., & Wu, L. (2000). Modeling climate shift of El Niño variability in the Holocene. *Geophysical Research Letters*, 27(15), 2265–2268. <https://doi.org/10.1029/2000GL011452>
- Liu, Z., Lu, Z., Wen, X., Otto-Bliesner, B. L., Timmermann, A., & Cobb, K. M. (2014). Evolution and forcing mechanisms of El Niño over the past 21,000 years. *Nature*, 515(7528), 550–553. <https://doi.org/10.1038/nature13963>
- McGregor, H. V., Fischer, M. J., Gagan, M. K., Fink, D., Phipps, S. J., Wong, H., & Woodroffe, C. D. (2013). A weak El Niño/Southern Oscillation with delayed seasonal growth around 4,300 years ago. *Nature Geoscience*, 6(11), 949–953. <https://doi.org/10.1038/geo1936>
- McGregor, S., Timmermann, A., England, M. H., Elison Timm, O., & Wittenberg, A. T. (2013). Inferred changes in El Niño–Southern Oscillation variance over the past six centuries. *Climate of the Past*, 9(5), 2269–2284. <https://doi.org/10.5194/cp-9-2269-2013>
- Moy, C. M., Seltzer, G. O., Rodbell, D. T., & Anderson, D. M. (2002). Variability of El Niño/Southern Oscillation activity at millennial timescales during the Holocene epoch. *Nature*, 420(6912), 162–165. <https://doi.org/10.1038/nature01194>
- Nurhati, I. S., Cobb, K. M., Charles, C. D., & Dunbar, R. B. (2009). Late 20th century warming and freshening in the central tropical Pacific. *Geophysical Research Letters*, 36, L21606. <https://doi.org/10.1029/2009GL040270>
- Otto-Bliesner, B. L., Brady, E. C., Fasullo, J., Jahn, A., Landrum, L., Stevenson, S., et al. (2015). Climate variability and change since 850 CE: An ensemble approach with the Community Earth System Model. *Bulletin of the American Meteorological Society*, 97(5), 735–754. <https://doi.org/10.1175/BAMS-D-14-00233.1>
- Otto-Bliesner, B. L., Brady, E. C., Shin, S.-I., Liu, Z., & Shields, C. (2003). Modeling El Niño and its tropical teleconnections during the last glacial-interglacial cycle. *Geophysical Research Letters*, 30(23), 2198. <https://doi.org/10.1029/2003GL018553>
- Power, S., Delage, F., Chung, C., Kociuba, G., & Keay, K. (2013). Robust twenty-first-century projections of El Niño and related precipitation variability. *Nature*, 502(7472), 541–545. <https://doi.org/10.1038/nature12580>
- Reynolds, R. W., Rayner, N. A., Smith, T. M., Stokes, D. C., & Wang, W. (2002). An improved in situ and satellite SST analysis for climate. *Journal of Climate*, 15(13), 1609–1625. [https://doi.org/10.1175/1520-0442\(2002\)015<1609:AIISAS>2.0.CO;2](https://doi.org/10.1175/1520-0442(2002)015<1609:AIISAS>2.0.CO;2)
- Rodbell, D. T., Seltzer, G. O., Anderson, D. M., Abbott, M. B., Enfield, D. B., & Newman, J. H. (1999). An ~15,000-year record of El Niño-driven alluviation in southwestern Ecuador. *Science*, 283(5401), 516–520. <https://doi.org/10.1126/science.283.5401.516>
- Sayani, H. R., Cobb, K. M., Cohen, A. L., Elliott, W. C., Nurhati, I. S., Dunbar, R. B., et al. (2011). Effects of diagenesis on paleoclimate reconstructions from modern and young fossil corals. *Geochimica et Cosmochimica Acta*, 75(21), 6361–6373. <https://doi.org/10.1016/j.gca.2011.08.026>
- Thompson, D. M., Conroy, J. L., Collins, A., Hlohowskyj, S. R., Overpeck, J. T., Riedinger-Whitmore, M., et al. (2017). Tropical Pacific climate variability over the last 6000 years as recorded in Bainbridge Crater Lake, Galápagos. *Paleoceanography*, 32, 903–922. <https://doi.org/10.1002/2017PA003089>
- Timmermann, A., Lorenz, S. J., An, S.-I., Clement, A., & Xie, S.-P. (2007). The effect of orbital forcing on the mean climate and variability of the Tropical Pacific. *Journal of Climate*, 20(16), 4147–4159. <https://doi.org/10.1175/JCLI4240.1>
- Wake, B. (2016). Snow white coral. *Nature Climate Change*, 6, 439. <https://doi.org/10.1038/nclimate3009>
- White, S. M., Ravelo, A. C., & Polissar, P. J. (2018). Dampened El Niño in the Early and Mid-Holocene due to insolation-forced warming/deepening of the thermocline. *Geophysical Research Letters*, 45, 316–326. <https://doi.org/10.1002/2017GL075433>
- Wilkinson, C. (Ed) (2004). *Status of coral reefs of the world*. Townsville, Australia: Australian Institute of Marine Science.
- Xie, P., & Arkin, P. A. (1997). Global precipitation: A 17-year monthly analysis based on gauge observations, satellite estimates, and numerical model outputs. *Bulletin of the American Meteorological Society*, 78(11), 2539–2558. [https://doi.org/10.1175/1520-0477\(1997\)078<2539:GPAYMA>2.0.CO;2](https://doi.org/10.1175/1520-0477(1997)078<2539:GPAYMA>2.0.CO;2)
- Zheng, W., Braconnot, P., Guilyardi, E., Merkel, U., & Yu, Y. (2008). ENSO at 6ka and 21ka from ocean–atmosphere coupled model simulations. *Climate Dynamics*, 30(7–8), 745–762. <https://doi.org/10.1007/s00382-007-0320-3>